Journal of Physiology (1992), **453**, *pp.* 413–434
With 10 figures
Printed in Great Britain

MYOPLASMIC FREE Mg^{2+} CONCENTRATION DURING REPETITIVE STIMULATION OF SINGLE FIBRES FROM MOUSE SKELETAL MUSCLE

BY HÅKAN WESTERBLAD AND DAVID G. ALLEN
From the Department of Physiology, F13, University of Sydney, NSW 2006, Australia

(*Received 15 August 1991*)

SUMMARY

1. The role of the myoplasmic free Mg^{2+} concentration ($[Mg^{2+}]_i$) in fatigue was studied in intact single fibres isolated from mouse skeletal muscle. Fatigue was produced by repeated tetanic stimulation. The fluorescent Mg^{2+} indicator furaptra was pressure injected into fibres. *In vivo* calibrations were performed to convert fluorescence signals into $[Mg^{2+}]_i$.

2. $[Mg^{2+}]_i$ at rest was $0{\cdot}78 \pm 0{\cdot}05$ mM (mean ± S.E.M., $n = 14$). An increase of the extracellular $[Mg^{2+}]$ from 0·5 to 20 mM resulted in a small elevation of $[Mg^{2+}]_i$ (86 μM in 5 min). Removal of extracellular Na^+ did not affect $[Mg^{2+}]_i$. An intracellular alkanization of about 0·6 pH units gave a $[Mg^{2+}]_i$ reduction of 65 μM.

3. During fatiguing stimulation $[Mg^{2+}]_i$ initially remained almost constant and it then suddenly started to rise towards the end of the stimulation period. The onset of the $[Mg^{2+}]_i$ rise was always followed by a rapid tension decline. In fatigue $[Mg^{2+}]_i$ was approximately twice as high as at rest.

4. Fibres were injected with $MgCl_2$ to study if the rise in $[Mg^{2+}]_i$ could explain the tension decline in fatigue. An elevation of $[Mg^{2+}]_i$ was accompanied by a tension reduction but the $[Mg^{2+}]_i$ for a given tension was generally much higher in rested fibres injected with $MgCl_2$ than in fatigued fibres. Thus the rise in $[Mg^{2+}]_i$ as such cannot explain the tension reduction in fatigue.

5. Injection of $MgCl_2$ was also used to assess the intracellular Mg^{2+} buffering. The mean Mg^{2+} buffer power (i.e. the ratio of the change in $[Mg^{2+}]_i$ to the amount of Mg^{2+} added) was 0·62.

6. ATP is the quantitatively most important binding site for Mg^{2+} at rest and ATP breakdown is then a likely source of the $[Mg^{2+}]_i$ increase in fatigue. The role of ATP breakdown in the increase of $[Mg^{2+}]_i$ was studied with metabolic inhibition: fibres were exposed to iodoacetic acid to inhibit glycolysis and cyanide to inhibit oxidative phosphorylation. The pattern during metabolic inhibition was similar to that observed during fatigue. After remaining almost constant during a lengthy period, $[Mg^{2+}]_i$ rose rapidly and this rise preceded a period of rapid tension decline. The fibres thereafter went into rigor and $[Mg^{2+}]_i$ stabilized at an elevated level; the mean $[Mg^{2+}]_i$ increase in rigor was 1·30 mM.

7. We have used modelling to determine the likely change in the intracellular ATP concentration ($[ATP]_i$) for the observed changes in $[Mg^{2+}]_i$. Our model could with

reasonable accuracy predict (i) the intracellular Mg^{2+} buffer power, (ii) the change in $[Mg^{2+}]_i$ due to an alkalinization, and (iii) the $[Mg^{2+}]_i$ increase in rigor.

8. The modelled $[ATP]_i$ for the average $[Mg^{2+}]_i$ in fatigue was 1·74 mM, which represents an $[ATP]_i$ reduction to about 30 % of the original. The time course of the $[Mg^{2+}]_i$ recovery after fatiguing stimulation suggests that a large fraction of the ATP which broke down during fatigue was deaminated to IMP (inosine monophosphate).

9. In conclusion, fatigue was associated with a marked increase of $[Mg^{2+}]_i$. This increase was, however, too small to explain the tension reduction in fatigue. A likely scenario is instead that the $[Mg^{2+}]_i$ increase reflects a breakdown of ATP and that this breakdown contributes to the tension decline in fatigue.

INTRODUCTION

Intracellular Mg^{2+} is likely to play a significant role in many cellular processes; for instance, in skeletal muscle cells Mg^{2+} will affect intracellular Ca^{2+} handling because (i) Mg^{2+} inhibits Ca^{2+} release from the sarcoplasmic reticulum (SR) (e.g. Meissner, Darling & Eveleth, 1986), (ii) Mg^{2+} inhibits the SR Ca^{2+} pumps (Krause, 1991), and (iii) Mg^{2+} competes with Ca^{2+} for binding sites on, for example, parvalbumin (e.g. Robertson, Johnson & Potter, 1981). Although Mg^{2+} is the most common myoplasmic divalent cation and exists in the millimolar range, it has proved difficult to measure the intracellular free concentration of Mg^{2+} ($[Mg^{2+}]_i$) and values reported for skeletal muscle vary more than tenfold (for brief review see Blatter, 1990). However, recent methodological advances have made it possible to measure $[Mg^{2+}]_i$ in individual cells with greater precision: a new type of magnesium-selective microelectrode with improved selectivity over interfering ions has become available (Hu, Bührer, Müller, Rusterholz, Rouilly & Simon, 1989) and a fluorescent Mg^{2+} indicator, furaptra, has been developed (Raju, Murphy, Levy, Hall & London, 1989). While microelectrode technique is well suited for measurements of $[Mg^{2+}]_i$ in muscle fibres at rest (Blatter, 1990; Günzel & Galler, 1991), this technique is difficult to use during contractions because of fibre movements. Thus it is more convenient to use furaptra to follow $[Mg^{2+}]_i$ during periods of contraction.

Previous studies of fatigue due to repeated tetanic stimulation of single mouse muscle fibres have shown that the tension reduction is caused by the combined effect of (i) reduced maximum Ca^{2+}-activated tension, (ii) reduced myofibrillar Ca^{2+} sensitivity, and (iii) reduced myoplasmic Ca^{2+} concentration ($[Ca^{2+}]_i$) during tetanus (Lännergren & Westerblad, 1991; Westerblad & Allen, 1991). An increase of the myoplasmic concentration of inorganic phosphate (P_i) is likely to be the dominant cause of (i) and (ii) (for discussion see Westerblad & Allen, 1992), whereas the cause of the declining tetanic $[Ca^{2+}]_i$ (iii), which occurs towards the end of fatiguing stimulation, remains unclear.

Lamb & Stephenson (1991) recently demonstrated that Mg^{2+} plays a key role in excitation–contraction coupling in skeletal muscle. These authors used skinned muscle fibres with intact voltage-sensor control of SR Ca^{2+} release and showed that 1 mM-Mg^{2+} (approximately the $[Mg^{2+}]_i$ of resting skeletal muscle cells (Blatter, 1990; Günzel & Galler, 1991)) inhibited SR Ca^{2+} release at rest, and this inhibition was overcome by depolarization. They also showed that an increase of the $[Mg^{2+}]$ concentration from 1 to 3 mM resulted in a marked reduction of the depolarization

induced SR Ca^{2+} release. A greater part of the total diffusible Mg^{2+} in the myoplasm ($\Sigma[Mg^{2+}]_i$) is bound to various intracellular binding sites of which ATP is the quantitatively most important in rested muscle (for review see Godt & Maughan, 1988). Since the intracellular concentration of ATP ($[ATP]_i$) has been shown to fall during fatiguing stimulation (for review see Vøllestad & Sejersted, 1988), it appears likely that $[Mg^{2+}]_i$ increases in fatigue and may reach a level where it inhibits SR Ca^{2+} release. To test this hypothesis, we have now used furaptra to measure $[Mg^{2+}]_i$ during fatigue.

Some of the present results have been presented in abstract form (Allen, Cairns & Westerblad, 1992).

METHODS

Male mice were killed by rapid neck disarticulation. Single muscle fibres were dissected from the flexor brevis muscle of the foot. After a fibre had been isolated, its tendons were gripped by platinum-foil micro-clips and the fibre was mounted between an Akers AE 801 force transducer and an adjustable holder allowing the fibre to be stretched to the length giving maximum tetanic tension. For a more comprehensive account of fibre dissection and mounting see Lännergren & Westerblad (1987).

The protocol for fatiguing stimulation has been described in detail previously (Lännergren & Westerblad, 1991). Briefly, fatigue was produced by intermittent tetanic stimulation which continued until tetanic tension was reduced to about 0·3 P_o (i.e. 30 % of the tension at the beginning of fatiguing stimulation). These periods of repeated tetani will be referred to as fatigue runs. At the start of fatigue runs tetani (350 ms, 100 Hz) were produced every 4 s and the tetanic interval was shortened by about 20 % every 2nd minute. A short pause ($\sim$ 10 s) was generally given each time the tetanic interval was changed and in most fibres also towards the end of fatiguing stimulation.

Tension recovery was followed in some experiments by giving test tetani at 1, 5, 10, 20 and 30 min after the end of fatiguing stimulation.

Values are presented as means ± S.E.M. Student's t test was used to verify statistical significance; the significance level was set at 0·05 throughout.

Solutions

Dissection was performed in the following solution (mM): NaCl, 136·5; KCl, 5·0; $CaCl_2$, 1·8; $MgCl_2$, 0·5; NaH_2PO_4, 0·4; $NaHCO_3$, 11·9. During experiments fibres were normally superfused by a standard Tyrode solution (mM): NaCl, 121; KCl, 5·0; $CaCl_2$, 1·8; $MgCl_2$, 0·5; NaH_2PO_4, 0·4; $NaHCO_3$, 24·0; glucose, 5·5; this solution was bubbled with 5 % CO_2 + 95 % O_2 which gave an extracellular pH (pH_o), measured close to the fibre, of 7·30. In some experiments the $[Mg^{2+}]_i$ response to a reduction or withdrawal of external Na^+ was studied. A HEPES-buffered solution was then used and Na^+ was replaced by Li^+ or tetramethylammonium ions (TMA^+) (mM): NaCl, LiCl or TMACl, 150; $CaCl_2$, 1·0; $MgCl_2$, 0·5; HEPES, 5·0; this solution was titrated with KOH to pH 7·3. About 0·2 % fetal calf serum was added to all the above solutions. All experiments were performed at room temperature (22 °C).

Injection of furaptra

In a few early experiments we tried to load fibres with furaptra (Mag-fura-2; Molecular Probes Inc., USA) in the membrane permeant acetoxymethyl (AM) ester form following a procedure previously used with Fura-2 (Westerblad & Allen, 1991). With AM loading the fibres became inexcitable and we have therefore instead injected the tetrapotassium salt of furaptra.

After a fibre had been mounted in the stimulation trough and a few test contractions, furaptra was introduced into the fibre by pressure injection. Furaptra was dissolved in 150 mM-KCl and 10 mM-HEPES (pH 7) at a concentration of 10 mM. About 1 μl of this solution was introduced into the back of a conventional, fibre-filled microelectrode (electrode resistances ranged from 30 to 100 MΩ). The electrode was placed in a holder which allowed pressure to be applied to the back of the electrode. The muscle fibre was penetrated while monitoring the membrane potential. When the microelectrode tip was inside the cell, the fibre was illuminated with fluorescent light (see below) and brief pulses of pressure were applied. The pressure was increased until clear injections were observed and approximately twenty brief pressure pulses were then applied.

The fibres were allowed to rest for about 1 h after the injections. Since we use fibres which are only about 0·6 mm long, this period of rest would allow furaptra to become homogeneously distributed along the fibre (cf. Konishi, Hollingworth, Harkins & Baylor, 1991).

Fluorescence measurements

The optical arrangements used to record the fluorescence signal have been described in detail previously (Lee, Westerblad & Allen, 1991). Briefly, a Nikon Diaphot microscope with a ×20 Fluor objective was used. The UV illumination was obtained from an Ealing Beck 150 W light source with a xenon arc lamp. Prolonged and intense illumination of fluorescent probes causes photobleaching which may affect measurements (Roe, Lemasters & Herman, 1990; Lee *et al.* 1991). To minimize photobleaching, a shutter was used to prevent illumination of the preparation except when required and a neutral density filter reduced the illuminating light 30 times. With these precautions no change of the fluorescence signal due to photobleaching could be detected. The fluorescence light, recorded from approximately 50% of the total length of a fibre, was guided to a photomultiplier tube and its amplified output (measured in nA or μA of photocathode current) was displayed on a pen recorder and stored on videotape.

The $[Mg^{2+}]_i$-dependent signal of furaptra was obtained by illuminating at 340 and 360 nm and dividing the resulting fluorescence signals emitted at 505 nm. The illuminating wavelength was automatically switched between 340 and 360 nm. The emitted light was passed to two sample and hold circuits so that the fluorescence signal at one illuminating wavelength was held when the other wavelength was in use. The two continuous signals obtained in this way were passed to an analogue divide circuit, whose output supplied a continuous 340/360 ratio signal; the initial 500 ms after each wavelength change was ignored by the divide circuit to avoid any artifact from filter movements and muscle contraction (see below). At rest the illuminating wavelength was changed every 4 s and during fatiguing stimulation the wavelength change was linked to stimulation so that contractions occurred during the initial 500 ms period when the fluorescence signal was ignored. In this way artifacts due to fibre movement were minimized and any contribution from the high tetanic $[Ca^{2+}]_i$ to the ratio signal was avoided (see below).

Besides the furaptra fluorescence signal, two other sources may contribute to the fluorescence light: (i) autofluorescence and (ii) background fluorescence.

(i) The autofluorescence was measured before injection of furaptra in twelve experiments. The autofluorescence was $7·7 \pm 0·5$ nA at 340 nm and $22·7 \pm 2·1$ nA at 360 nm which at both wavelengths is less than 1% of the average signal after injection. Thus autofluorescence did not substantially affect the light signal and has been ignored.

(ii) The background fluorescence, measured at regular intervals by moving the fibre out of the field of view, was found to be small (< 10% of the total fluorescence) and remained virtually constant throughout experiments. By adjusting the input zero level of the divide circuit, background fluorescence has been subtracted from the signals used to produce the ratio.

The intracellular concentration of furaptra was assessed by comparing the fluorescence of injected fibres with that from glass capillaries which had the same inner diameter as a normal fibre and contained known concentrations of furaptra. The mean intracellular furaptra concentration was found to be $\sim 100\ \mu$M.

Calibration of furaptra fluorescence signals

We have performed both *in vivo* and *in vitro* calibrations of the furaptra signals. The *in vitro* calibration was performed by adding various amounts of $MgCl_2$ to a solution of the following composition: KCl, 150 mM; HEPES, 10 mM; EGTA, 100 μM; furaptra, 2·5 μM; pH 7·0. In a few early attempts no EGTA was added to the solution and this resulted in high ratios without obvious relation to the $[Mg^{2+}]$ concentration. This was most likely due to interference with Ca^{2+} and possibly also other divalent cations (cf. Konishi *et al.* 1991). Figure 1*A* summarizes the results from *in vitro* calibrations. It is well established that changes of the ionic strength affect the response of fluorescent indicators (e.g. Williams & Fay, 1990) and this will create a potential problem at high $[Mg^{2+}]$ concentrations; for example, addition of 50 mM-$MgCl_2$, which was the highest concentration used, will approximately double the ionic strength of our calibration solution and to fully compensate for this all KCl should be removed. This would not occur in our *in vivo* calibration, where the osmotic rather than the ionic strength would remain constant (see below). We have used both the standard 150 mM-KCl and, to keep the osmolarity constant, 75 mM-KCl in the calibration solution with 50 mM-$MgCl_2$. The difference in fluorescence signal obtained with these two solutions was small: the 340/360 ratio was about 5% higher with 75 mM-KCl.

The effect of pH on the ratio signal was tested in one experiment: the ratio at 2 mM-Mg^{2+} was not noticeably affected by a pH change from 6·5 to 7·5. Since this pH change is markedly larger than that occurring in our fibres during fatiguing stimulation (Westerblad & Allen, 1992), altered pH will not affect the $[Mg^{2+}]_i$ measurements.

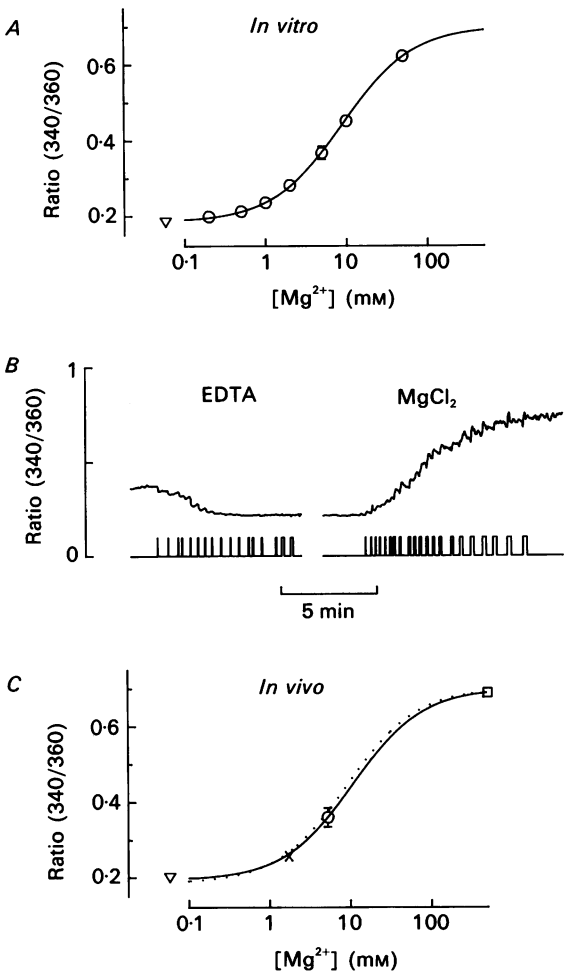

Fig. 1. *In vitro* and *in vivo* calibration of furaptra. *A* shows a summary of the *in vitro* calibrations. The data points were obtained in zero Mg^{2+} (▽) and after addition of various amounts of $MgCl_2$ (○). The curve was constructed by fitting data points with eqn (1). *B* shows fluorescence ratio records from one *in vivo* calibration experiment. R_{min} was first established by injection of 0·5 M-K_2EDTA and R_{max} was thereafter approached by injecting 0·5 M-$MgCl_2$. Periods of injection are indicated below records; note that each injection resulted in a clear change of the ratio until a stable low or high level was obtained. *C* summarizes the *in vivo* calibrations. ▽ and □ represent injection with 0·5 M-K_2EDTA ($n = 5$) and 0·5 M-$MgCl_2$ ($n = 5$), respectively. The intermediate points were obtained by injection of magnesium tartronate (○, $n = 4$) and magnesium oxalate (×, $n = 1$). The curve was drawn according to eqn (1) and is compared with the *in vitro* calibration curve (dotted line). Data points (open symbols) in *A* and *C* represent means ± S.E.M. (error bars in most cases smaller than symbols).

The relation between 340/360 ratios and $[Mg^{2+}]$ was assessed according to Grynkiewicz, Poenie & Tsien (1985) and the curve in Fig. 1*A* was drawn using the equation:

$$[Mg^{2+}] = K_D[(R-R_{min})/(R_{max}-R)]S_{f2}/S_{b2}, \quad (1)$$

where R is the 340/360 ratio at a given $[Mg^{2+}]$. R_{min}, the ratio obtained in a solution with no added $MgCl_2$, was $0{\cdot}19 \pm 0{\cdot}002$ ($n = 10$). R_{max}, the ratio at infinite $[Mg^{2+}]$, was chosen to be 0·70 which gave the best fit between the curve and the measurements at intermediate $[Mg^{2+}]$. S_{f2} and S_{b2} are constants representing the fluorescence levels with 360 nm illumination at zero and infinite $[Mg^{2+}]$, respectively. S_{f2} was obtained in a solution with no added $MgCl_2$ and S_{b2} was obtained by multiplying the 360 nm fluorescence signal at 50 mM-$MgCl_2$ by 1·1 to compensate for the difference between the fluorescence ratio at 50 mM-Mg^{2+} and R_{max}; consecutive estimates of S_{f2} and S_{b2} on four occasions gave an S_{f2}/S_{b2} of $2{\cdot}37 \pm 0{\cdot}05$. Using the above mean values, the apparent Mg^{2+} dissocation constant, K_D, of furaptra was 3·80 mM. This value of K_D lies between values previously obtained at 37 °C (1·5 mM; Raju *et al.* 1989) and 16·5 °C (5·3 mM; Konishi *et al.* 1991).

In a few early attempts to obtain an *in vivo* calibration, the ionophore ionomycin was used to equilibrate the $[Mg^{2+}]$ across the cell membrane, but this did not give satisfactory results (cf. Raju *et al.* 1989). We have instead employed another method: pressure injection of solutions with (i) EDTA, a Mg^{2+} chelator, (ii) high $[Mg^{2+}]$, and (iii) $[Mg^{2+}]$ buffered to an intermediate level. Figure 1*B* shows records from one *in vivo* calibration experiment. R_{min} was established by injecting 0·5 M-K_2EDTA, which has a K_D for Mg^{2+} of 1·67 μM (Martell & Smith, 1974) and consequently will reduce $[Mg^{2+}]_i$ to close to zero when in excess. K_2EDTA injections were given until clear injections no longer caused a reduction of the fluorescence ratio. After assessing R_{min}, the fibre was injected with 0·5 M-$MgCl_2$ to obtain a ratio at high $[Mg^{2+}]_i$. R_{min} was established in five experiments and had a mean of 0·19 (±0·01; ▽ in Fig. 1*C*). The ratio at 0·5 M-Mg^{2+} was $0{\cdot}69 \pm 0{\cdot}01$ ($n = 5$; □ in Fig. 1*C*); the R_{max} used to construct the *in vivo* calibration curve has been set at 0·70. It may be noted that while it is likely that water crossed the sarcolemma to keep the osmotic strength constant during the period of injections (a marked fibre swelling was observed), the ionic strength must have increased with each injection because both magnesium and EDTA ions are divalent. A plateau was obtained both with injection of K_2EDTA and $MgCl_2$ despite increasing ionic strength and consequently the properties of furaptra cannot have been significantly affected by ionic strength.

The *in vivo* S_{f2}/S_{b2} was obtained from the 360 nm signals obtained with injection of K_2EDTA and $MgCl_2$, respectively, after compensating for a general decline of the emitted light with time. The S_{f2}/S_{b2} assessed in this way was $2{\cdot}33 \pm 0{\cdot}07$ ($n = 4$).

To obtain a data point between R_{min} and R_{max}, and consequently get a measure of the *in vivo* K_D, we have used substances with a Mg^{2+} K_D in the low millimolar range and, to avoid interference with Ca^{2+}, weak Ca^{2+} binding. We initially used oxalate (pH 7 with KOH) mixed with $MgCl_2$ to give an oxalate to magnesium oxalate ratio of 1. The *in vitro* established Mg^{2+} K_D of the oxalate solution was 1·72 mM which is similar to the K_D reported in the literature (Martell & Smith, 1974). A serious problem with the oxalate solution was that it easily precipitated and plugged the electrode during injection and obvious injections of this solution were only obtained in one experiment (× in Fig. 1*C*). In later experiments we instead used tartronate; the *in vitro* established Mg^{2+} K_D of tartronate was 5·25 mM, which is slightly lower than previously reported (Martell & Smith, 1974). A solution containing 250 mM-tartronate (pH 7 with KOH) and 125 mM-$MgCl_2$ was used for injections; this solution also contained 100 μM-EGTA to avoid interference from Ca^{2+}. As for establishing R_{min} and R_{max}, the tartronate solution was injected until further injection no longer changed the fluorescence ratio. Starting from the resting $[Mg^{2+}]_i$, a plateau was reached in four experiments and the ratio at this point was $0{\cdot}36 \pm 0{\cdot}03$ (○ in Fig. 1*C*).

Figure 1*C* summarizes the calibration experiments and shows both the *in vivo* (continuous line) and *in vitro* (dotted line) calibration curves. The following values of the parameters of eqn (1) have been used to construct the *in vivo* and *in vitro* curves, respectively: $R_{min} = 0{\cdot}19$ and 0·19; $R_{max} = 0{\cdot}70$ and 0·70; $S_{f2}/S_{b2} = 2{\cdot}33$ and 2·37; K_D 4·60 and 3·80. Thus the difference between values obtained *in vivo* and *in vitro* was small ($\leqslant 10\%$) with the exception of K_D. The higher K_D *in vivo* may be explained by the binding of furaptra to myoplasmic proteins (cf. Konishi, Olson, Hollingworth & Baylor, 1988).

The *in vivo* calibration curve has been used to convert fluorescence ratios to $[Mg^{2+}]_i$. The ratios were measured from pen records to the nearest 0·001, which means that the smallest detectable change of $[Mg^{2+}]_i$ was about 50 μM.

At room temperature furaptra is about 100 times more sensitive to Ca^{2+} than to Mg^{2+} (Konishi *et al.* 1991). The resting $[Ca^{2+}]_i$ of our fibres is about 30 nM and in fatigue it has increased to about 100 nM (Westerblad & Allen, 1991). This rise in $[Ca^{2+}]_i$ would increase the furaptra fluorescence ratio corresponding to a $[Mg^{2+}]_i$ increase of 7 μM ((100 − 30 nM) × 100) and hence the rise of resting $[Ca^{2+}]_i$ in fatigue will not significantly affect $[Mg^{2+}]_i$ measurements. During tetanic stimulation

TABLE 1. Apparent binding constants and resting values of total concentrations used for $[Mg^{2+}]_i$ modelling (pH 7·3, 22 °C)

Species	Apparent binding constants (M^{-1})	Species	Total concentration (mM)
CaATP	$6{\cdot}06 \times 10^3$	K	150
MgATP	$1{\cdot}35 \times 10^4$	Na	10
KATP	5·22	PCr	25
NaATP	7·01	ATP	6
CaPCr	14·1	ADP	5×10^{-3}
MgPCr	19·9	AMP	4×10^{-6}
CaP_i	37·4	P_i	4
MgP_i	56·7	Parvalbumin	0·43
KP_i	2·31	Troponin	0·07
NaP_i	2·97		
Ca-parvalbumin*	$4{\cdot}50 \times 10^8$		
Mg-parvalbumin*	$3{\cdot}70 \times 10^4$		
MgAMP	43·0		
CaADP	498		
MgADP	766		
MgIMP	102		

* The same binding constants were used for the Ca^{2+}–Mg^{2+} sites on troponin.

$[Ca^{2+}]_i$ increases to about 1 μM (Westerblad & Allen, 1991) which corresponds to an increase of $[Mg^{2+}]_i$, as reported by furaptra, of 100 μM. Thus tetanic $[Ca^{2+}]_i$ is high enough to significantly affect the furaptra ratio signal and the periods of tetanic stimulation have therefore been excluded from the continuous ratio measurements during fatigue runs (see above).

Mg^{2+} buffering

The intracellular Mg^{2+} buffer power was assessed by injecting a mixture of 250 mM-$MgCl_2$ and 5 mM-furaptra. The rise of the fluorescence signal was used to establish the increase in the intracellular furaptra concentration from which the amount of Mg^{2+} added ($\Delta\Sigma[Mg^{2+}]_i$) was calculated. The Mg^{2+} buffer power will then be the ratio of the observed change of $[Mg^{2+}]_i$ ($\Delta[Mg^{2+}]_i$) to the amount of Mg^{2+} added, i.e.:

$$\text{buffer power} = \Delta[Mg^{2+}]_i / \Delta\Sigma[Mg^{2+}]_i. \quad (2)$$

Sizeable injections were required to get a reliable measure of the increase in furaptra concentration and injections which elevated the furaptra concentration less than 5 μM (corresponding to a $\Delta\Sigma[Mg^{2+}]_i$ of 0·25 mM) were disregarded.

Modelling of $[Mg^{2+}]_i$

Our results show that movements of Mg^{2+} across the sarcolemma are slow (see below). This suggests that rapid changes in $[Mg^{2+}]_i$ represent redistribution of Mg^{2+} between various intracellular binding sites and the pool which is free in the myoplasm. Based on the approach of Godt & Maughan (1988), we have constructed a model which includes the main intracellular Mg^{2+} binding sites. The apparent binding constants (22 °C, pH 7·3) of all the species which are included in the model are shown in Table 1; the values used were obtained from Fabiato (1988) and Curtin & Woledge (1978; their Table 4). The relation between $[Mg^{2+}]_i$ and $\Sigma[Mg^{2+}]_i$ was modelled using the programs described by Fabiato (1988). To explore the changes in $[Mg^{2+}]_i$ which occur in fatigue and

rigor, we assume that $\Sigma[Mg^{2+}]_i$ remains unchanged as phosphocreatine (PCr) and ATP are gradually degraded to creatine (Cr), AMP and P_i. The following concentrations of phosphorus compounds were used for resting conditions (mM): PCr, 25; ATP, 6; P_i, 4 (Leijendekker & Elzinga, 1990); complete breakdown of PCr and ATP was assumed to give (mM): AMP, 6; P_i 41. Intermediate concentrations of ATP, ADP, AMP, PCr and P_i were calculated on the assumption that as ATP and PCr were degraded, the Lohmann reaction (PCr + ADP $\Leftrightarrow$ Cr + ATP) and the myokinase reaction (2ADP $\Leftrightarrow$ ATP + AMP) remained at equilibrium. Details of this approach are given in Allen & Orchard (1987), which also shows the relationship between these species graphically. Accumulation of inosine monophosphate (IMP) due to deamination of AMP is known to occur in fatigue (e.g. Sahlin, Palmskog & Hultman, 1978). For simplicity this has not been taken into account in the basic model; the effect of increased IMP in fatigue was, however, studied in separate modelling experiments (see Discussion). The Mg^{2+} binding of Cr is negligible and has been ignored. Intracellular pH (pH_i) was assumed constant at 7·3 throughout fatigue runs (Westerblad & Allen, 1992) and also throughout periods of metabolic blockade which eventually caused rigor development. Accumulation of lactate in fatigue was ignored as trial calculations showed negligible effect on $[Mg^{2+}]_i$. The basic model was simplified in that $[Ca^{2+}]_i$ was held constant at 30 nM, the resting $[Ca^{2+}]_i$ in these fibres (Westerblad & Allen, 1991), throughout periods of fatiguing stimulation and metabolic blockade. The resting $[Ca^{2+}]_i$ rises to about 100 nM in fatigue (Westerblad & Allen, 1991) and the effect of this rise on $[Mg^{2+}]_i$ was determined with modelling (see Discussion). Parvalbumin and troponin have two high-affinity, Ca^{2+}–Mg^{2+} binding sites each. The properties of these binding sites are very similar (e.g. Robertson *et al.* 1981) and they have therefore been treated as one unit. The parvalbumin concentration of the present preparation is about 0·43 mM (Westerblad & Lännergren, 1991) and the troponin concentration was assumed to be 70 μM, thus together they contain 1 mM-Ca^{2+}–Mg^{2+} binding sites.

The effect of CO_2 removal from the bath solution was modelled assuming a pH_i change from 7·3 to 7·9 (Westerblad & Allen, 1992). The apparent binding constants of all pH-sensitive species in Table 1 were then recalculated for pH 7·9 and the change in $[Mg^{2+}]_i$ was modelled assuming constant $\Sigma[Mg^{2+}]_i$.

RESULTS

Regulation of $[Mg^{2+}]_i$ at rest

The resting $[Mg^{2+}]_i$ of fourteen fibres was 0·78 ± 0·05 mM. This is about 100 times less than what would be expected if $[Mg^{2+}]_i$ was in electrochemical equilibrium and hence Mg^{2+} extruding mechanisms must exist.

The role of the extracellular $[Mg^{2+}]$ ($[Mg^{2+}]_o$) on $[Mg^{2+}]_i$ was assessed in five fibres and one typical example is shown in Fig. 2*A*. Increasing $[Mg^{2+}]_o$ from 0·5 to 20 mM resulted in a small, but significant, increase of $[Mg^{2+}]_i$: exposure to the high Mg^{2+} solution for 5 min caused a $[Mg^{2+}]_i$ increase of 86 ± 24 μM ($n = 5$).

It has been suggested that Na^+–Mg^{2+} exchange may contribute to the low $[Mg^{2+}]_i$ (Baker & Crawford, 1972; Blatter, 1990). The importance of Na^+–Mg^{2+} exchange was tested by substituting the extracellular Na^+ with TMA^+. Figure 2*B* shows one such experiment and in this case $[Mg^{2+}]_i$ remained almost unchanged when the bath solution was changed to a solution with zero Na^+ and 10 mM-Mg^{2+}. Similar results were obtained in another experiment where Na^+ was completely replaced by TMA^+ and also in one experiment where the bath Na^+ concentration was reduced to 10 mM by substitution with Li^+.

Changes of pH_i may affect $[Mg^{2+}]_i$, for example by competition between H^+ and Mg^{2+} for intracellular binding sites. The role of changed pH_i on $[Mg^{2+}]_i$ was studied in four fibres and one of these experiments is shown in Fig. 2*C*. The external fluid was here changed from the standard Tyrode solution, bubbled with 5% CO_2, to the solution used during dissection, which was not bubbled. This procedure, which causes

an intracellular alkalinization of about 0·6 pH units (Westerblad & Allen, 1992), resulted in a significant $[Mg^{2+}]_i$ reduction of 65 ± 15 μM ($n = 4$).

The rate of $[Mg^{2+}]_i$ recovery after $MgCl_2$ injections was studied in six fibres. During the first few minutes after the injection there was a relatively fast decline of $[Mg^{2+}]_i$.

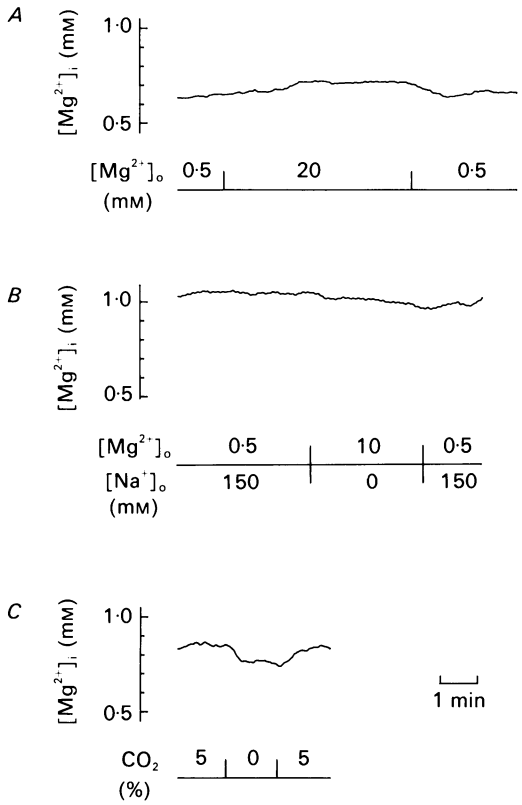

Fig. 2. The effect on $[Mg^{2+}]_i$ of altered extracellular solution. The records were obtained from three different fibres; the ionic change and its timing are indicated below each record. In *A* $[Mg^{2+}]_o$ was increased from 0·5 to 20 mM by adding $MgCl_2$. In *B* extracellular Na^+ was replaced by TMA^+ and $[Mg^{2+}]_o$ increased from 0·5 to 10 mM. In *C* an intracellular alkalinization was produced by removal of CO_2. The time bar in *C* refers to all three traces.

Since injection and measurement were performed in the same part of the fibre, this rapid decline probably represents diffusion of Mg^{2+} from the injection site. After this initial phase, recovery of $[Mg^{2+}]_i$ was very slow and it generally had a half-time ($t_{0.5}$) of more than 1 h. To get a quantitative measure of the rate of Mg^{2+} extrusion after injection, we measured the slope of $[Mg^{2+}]_i$ decline between 10 and 20 min after injection and it was $12 \pm 2{\cdot}8$ μM/min ($n = 6$) starting from a mean $[Mg^{2+}]_i$ of 2·2 mM.

$[Mg^{2+}]_i$ *in fatigue*

The tension decline during fatigue runs occurs in a characteristic way in the present preparation. Initially tension falls to about 0·85 P_0 in ten tetani (phase 1), then follows a lengthy period of almost stable tension production, the duration of

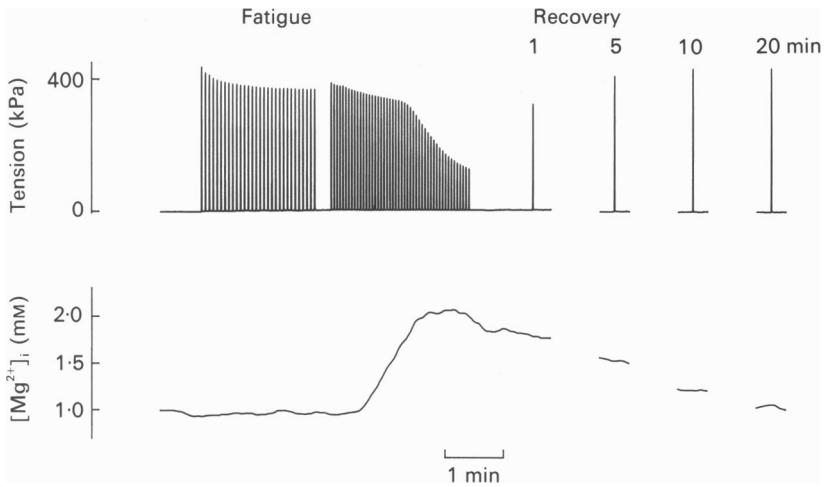

Fig. 3. Tension and $[Mg^{2+}]_i$ records obtained from one fibre during a fatigue run and the subsequent recovery period. Each vertical line in the tension record represents a tetanic contraction. Timing of tetanic stimulation during recovery is indicated above each tetanus.

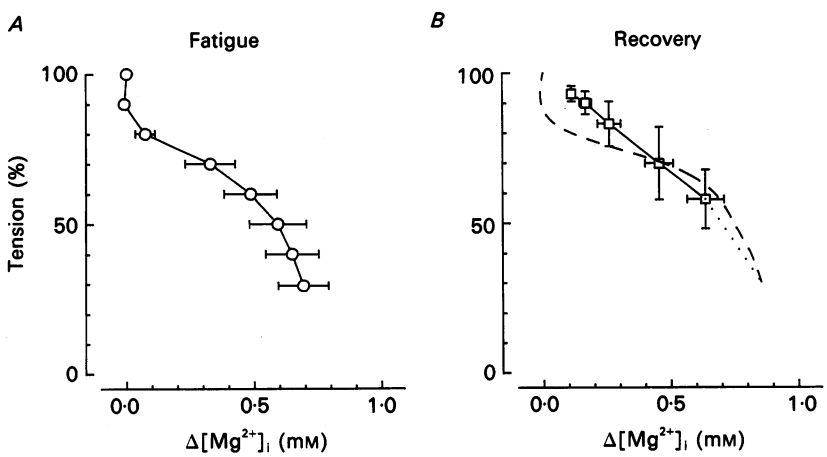

Fig. 4. The relation between $\Delta[Mg^{2+}]_i$ and tetanic tension obtained during fatiguing stimulation and recovery. The fatigue data points in *A* were obtained from nine fibres at the start, at each 10 % tension reduction down to 0·4 P_o, and finally at the end of fatigue runs. The recovery data points in *B* were obtained from four fibres at 1, 5, 10, 20 and 30 min after the end of fatiguing stimulation; dashed line connects mean values obtained from the same fibres during fatiguing stimulation.

which depends on the fatigue resistance (phase 2), and finally tension declines rapidly (phase 3) (Lännergren & Westerblad, 1991). Figure 3 shows records of tension and $[Mg^{2+}]_i$ obtained from a fibre during a fatigue run and the subsequent recovery period. This fibre, which was relatively easily fatigued, displayed the characteristic tension decline with three phases. $[Mg^{2+}]_i$ remained virtually constant during phase

1 and the beginning of phase 2. Towards the end of phase 2, $[Mg^{2+}]_i$ suddenly started to rise and at the end of the fatigue run it was approximately doubled. Similar results were obtained in eight more fibres studied during fatiguing stimulation and the results are summarized in Fig. 4*A*, where $\Delta[Mg^{2+}]_i$ has been plotted against tetanic

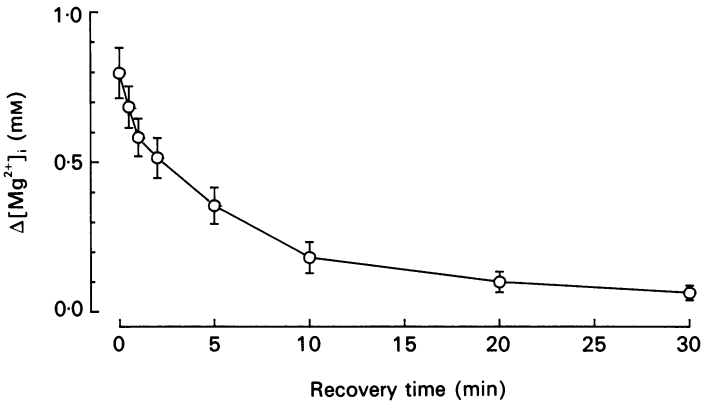

Fig. 5. Recovery of $[Mg^{2+}]_i$ after fatigue runs. Measurements performed in seven fibres.

tension. The mean $[Mg^{2+}]_i$ increased from 0·86 to 1·55 mM during fatigue runs which gives an increase in fatigue of $0{\cdot}69 \pm 0{\cdot}10$ mM ($n = 9$).

The rate of $[Mg^{2+}]_i$ recovery after fatigue runs was studied in seven fibres and the results are summarized in Fig. 5. The initial rate of $[Mg^{2+}]_i$ recovery was fast and it then became successively slower as recovery progressed. Thus $[Mg^{2+}]_i$ recovery could not be described by a monoexponential curve which suggests that the recovery involved more than one process.

Recovery of both tetanic tension and $[Mg^{2+}]_i$ was studied in the fibre depicted in Fig. 3 and in three more fibres and the results are summarized in Fig. 4*B*. It can be seen that there was an almost linear relation between recovery of tension and $[Mg^{2+}]_i$. The data points obtained during recovery also lie close to those obtained from the same fibres during fatiguing stimulation (represented by the dashed line).

Stimulation was stopped for about 10 s during the final part of six fatigue runs. After the pause the mean tetanic tension had increased from 0·29 to 0·53 P_0 and the mean $[Mg^{2+}]_i$ declined by 120 μM. When values obtained from these 10 s recovery periods were plotted in the same way as in Fig. 4*B* (result not shown), they were found to lie very close to the curve obtained during fatiguing stimulation. To sum up, the relationship between tension and $[Mg^{2+}]_i$ obtained during recovery is similar to that during fatiguing stimulation.

Metabolic inhibition

Since ATP is the quantitatively most important binding site for Mg^{2+} in rested muscle, a reduction of $[ATP]_i$ is a likely explanation for the increase of $[Mg^{2+}]_i$ in fatigue. To further study the role of reduced $[ATP]_i$ for the increase in $[Mg^{2+}]_i$, we have exposed fibres to a solution which will inhibit the two major ATP generating

pathways: iodoacetic acid (IAA) was used to block glycolysis and cyanide (CN) inhibited oxidative phosphorylation. Figure 6 shows records from one metabolic inhibition experiment. The fibre was stimulated to produce a tetanus every minute and the pattern of tension decline *vs.* $[Mg^{2+}]_i$ increase observed was similar to that

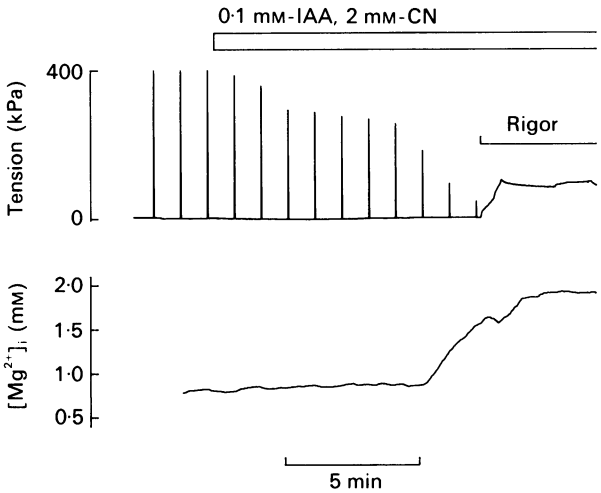

Fig. 6. Tension and $[Mg^{2+}]_i$ records from a metabolic blockade experiment. Application of IAA and CN indicated above tension record. Vertical lines in tension record represent tetanic contractions which were produced every minute; the fibre did not respond to electrical stimulation after development of rigor.

during fatigue runs. When the fibre was exposed to IAA and CN, tension initially declined and thereafter it remained almost constant for a few minutes; $[Mg^{2+}]_i$ did not show any marked increase during this period. Thus this initial period resembles phase 1 and the first part of phase 2 during fatigue runs. After about 7 min with metabolic inhibition, tetanic tension started to fall more rapidly and $[Mg^{2+}]_i$ began to rise at approximately the same time; thus this period shows similarities with the final part of phase 2 and phase 3 in fatigue. Eventually the fibre went into rigor and electrical stimulation no longer resulted in any tension increase. The rate of $[Mg^{2+}]_i$ increase became slower when rigor occurred and after a few minutes $[Mg^{2+}]_i$ remained stable at an elevated level. Similar results were obtained in two more fibres and the mean $[Mg^{2+}]_i$ increased from 0·78 mM at rest to 2·08 mM in rigor, thus giving a $\Delta[Mg^{2+}]_i$ of $1{\cdot}30 \pm 0{\cdot}16$ mM ($n = 3$).

Injection of $MgCl_2$

There was a temporal correlation between the final, rapid tension decline and the rise of $[Mg^{2+}]_i$ in both fatigue and metabolic blockade. In an attempt to study if the marked tension reduction was caused by the increase of $[Mg^{2+}]_i$ as such, rested fibres were injected with $MgCl_2$ so that the tetanic tension at various $[Mg^{2+}]_i$ could be measured. Most fibres were either inexcitable or produced a very low tension immediately after injection of $MgCl_2$. We attribute this inhibition to a brief

membrane depolarization caused by the injection. After this short phase of almost complete inactivation, tension normally increased gradually up to a stable level; experiments in which no stable tension level was obtained after injection have been excluded.

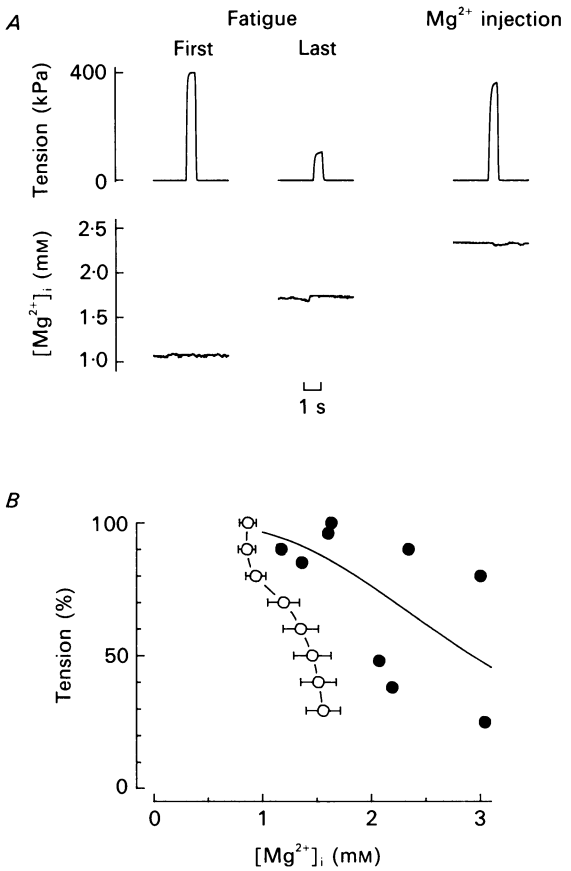

Fig. 7. Tetanic tension *vs.* $[Mg^{2+}]_i$ in fatigue and after injection of $MgCl_2$. Original records obtained in one experiment are shown in *A*. Note that almost maximum tension was produced after $MgCl_2$ injection although $[Mg^{2+}]_i$ was markedly higher than in fatigue. *B* shows data points obtained from nine $MgCl_2$ injection experiments on six fibres (●). These points are compared with points representing the mean (±S.E.M.) from all nine fatigue runs (○). The continuous line was obtained by fitting points obtained with injection to a Hill plot where the $[Mg^{2+}]_i$ at 0·5 P_o = 2·9 mM.

Figure 7*A* shows records from one experiment which clearly indicates that increased $[Mg^{2+}]_i$ was not the cause of the tension reduction. The $[Mg^{2+}]_i$ after $MgCl_2$ injection was in this case 2·34 mM which compares to 1·83 mM in fatigue. Despite the markedly higher $[Mg^{2+}]_i$ after injection the tension was 0·9 P_o, whereas it was only 0·3 P_o in fatigue.

The effect of increased $[Mg^{2+}]_i$ on tetanic tension was studied in six fibres and the results are summarized in Fig. 7*B*. It can be seen that the data points obtained with

$MgCl_2$ injection (●) lie markedly to the right of points obtained during fatigue runs (○). Thus, the $[Mg^{2+}]_i$ at a given tension was generally markedly higher in the rested state as compared to fatigue.

Mg^{2+} buffering: measured and modelled

The intracellular Mg^{2+} buffering was assessed in six experiments by injecting a mixture of $MgCl_2$ and furaptra. Figure 8 summarizes these experiments and it also

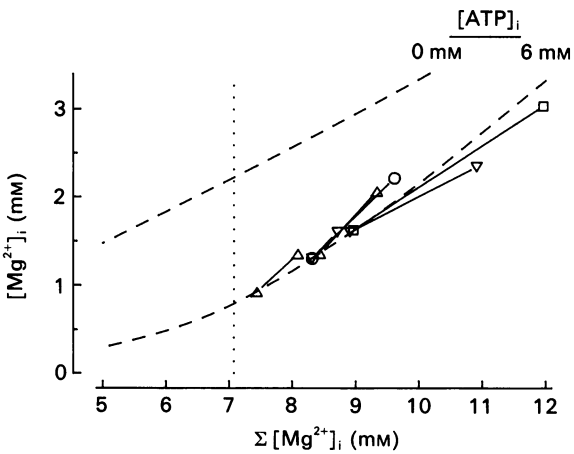

Fig. 8. Mg^{2+} buffering: measured and modelled. The change in $[Mg^{2+}]_i$ due to injection of $MgCl_2$ was studied in six experiments on four fibres (open symbols; each fibre has its own symbol). Pre-injection data points were placed on the lower dashed line which represents the modelled relation between $\Sigma[Mg^{2+}]_i$ and $[Mg^{2+}]_i$ at 6 mM-ATP. The upper dashed line shows the modelled $\Sigma[Mg^{2+}]_i$–$[Mg^{2+}]_i$ relationship at zero ATP. The dotted line indicates the $\Sigma[Mg^{2+}]_i$ which gives the mean resting $[Mg^{2+}]_i$.

shows the relation between $\Sigma[Mg^{2+}]_i$ and $[Mg^{2+}]_i$ as predicted by the model (see Methods) at 0 and 6 mM-ATP. The data points representing pre-injection values have been placed on the line given by the model for 6 mM-ATP, which is assumed to be the $[ATP]_i$ at rest. It can be seen that the relation between $\Delta\Sigma[Mg^{2+}]_i$ and $\Delta[Mg^{2+}]_i$ obtained with injections is similar to that predicted by the model: Mg^{2+} injections gave a mean buffer power of 0·62 and the buffer power predicted by the model for the same $\Sigma[Mg^{2+}]_i$ range (7–12 mM) was about 0·5.

DISCUSSION

The development of ion-sensitive, fluorescent indicators has made it possible to follow the cytosolic concentration of various ions with good time resolution during periods of contraction. Thus these indicators are valuable tools in studies of skeletal muscle fatigue. We have now employed a recently developed Mg^{2+}-sensitive indicator, furaptra, to measure $[Mg^{2+}]_i$ during fatigue produced by repeated tetanic stimulation of single muscle fibres from the mouse. The smallest detectable change

of $[Mg^{2+}]_i$ was about 50 μM which compares with a mean $\Delta[Mg^{2+}]_i$ in fatigue of 0·69 mM. It was possible to perform *in vivo* calibrations which gave consistent measures of the fluorescence ratio at zero, intermediate and high $[Mg^{2+}]_i$.

Resting $[Mg^{2+}]_i$

We report a mean resting $[Mg^{2+}]_i$ of 0·78 mM. This is similar to values recently obtained in frog muscle with a novel, improved type of Mg^{2+}-sensitive microelectrode (0·93 mM, Blatter, 1990; 1·3 mM, Günzel & Galler, 1991). Further, MacDermott (1990) obtained a resting $[Mg^{2+}]_i$ of 0·47 mM in rat extensor digitorum muscle with the old type of Mg^{2+}-sensitive microelectrode; this value was obtained after correction for interference from Na^+ and K^+ whose activities were measured in the same preparation. Thus with recently improved techniques, measurements of $[Mg^{2+}]_i$ in resting skeletal muscle cluster around 1 mM and mammalian muscle seems to have a somewhat lower $[Mg^{2+}]_i$ than frog muscle.

Resting $[Mg^{2+}]_i$ is about 100 times smaller than predicted by a simple Nernstian equilibrium and hence some kind of Mg^{2+} extruding mechanism(s) must exist. We observed a mean $[Mg^{2+}]_i$ increase of 86 μM over 5 min when $[Mg^{2+}]_o$ was elevated from 0·5 to 20 mM. When similar experiments were performed by Blatter (1990) in frog muscle, a much larger increase in $[Mg^{2+}]_i$ was obtained (about 500 μM) and this increase was accompanied by a fall of the intracellular Na^+ concentration. Blatter also observed a large increase of $[Mg^{2+}]_i$ when the extracellular Na^+ was removed. Based on these findings, he proposed that Na^+–Mg^{2+} exchange was involved in maintaining $[Mg^{2+}]_i$ at a low level. We did not observe any significant change of $[Mg^{2+}]_i$ in response to a reduction or removal of extracellular Na^+. Thus when compared to frog muscle, the flux of Mg^{2+} across the sarcolemma appears to be slower and Na^+–Mg^{2+} exchange was not apparent on the time scale of our experiments.

The small change in $[Mg^{2+}]_i$ which occurred when $[Mg^{2+}]_o$ was raised 40-fold could either arise because regulation of $[Mg^{2+}]_i$ is very active or because Mg^{2+} entry is slow. The experiments with $MgCl_2$ injection support the latter alternative: after an initial rapid fall of the measured $[Mg^{2+}]_i$, which probably represents diffusion of Mg^{2+} from the site of injection, the rate of $[Mg^{2+}]_i$ decline was very slow ($t_{0.5} > 1$ h). Between 10 and 20 min after injection $[Mg^{2+}]_i$ declined at a rate of 12 μM/min. Taking the Mg^{2+} buffer power (0·62) into account, this gives a Mg^{2+} efflux rate of only 19 μM/min.

We found that an intracellular alkalinization of about 0·6 pH units gave a mean $[Mg^{2+}]_i$ reduction of 65 μM. A likely explanation for this finding is that H^+ and Mg^{2+} compete for intracellular binding sites. We have used the model described in Methods to test this hypothesis. For a pH_i increase from 7·3 to 7·9 the model predicts a $[Mg^{2+}]_i$ reduction of 50 μM. Thus the modelled $[Mg^{2+}]_i$ reduction is similar to the measured reduction, which supports the proposal that the $[Mg^{2+}]_i$ decline was due to intracellular redistribution of H^+ and Mg^{2+}.

$[Mg^{2+}]_i$ *in fatigue*

$[Mg^{2+}]_i$ described a characteristic pattern during fatigue runs: initially it remained almost constant and it then rose rapidly towards the end of fatigue runs. This pattern would be predicted if ATP is the main Mg^{2+} source and if the Lohmann and myokinase reactions remain at equilibrium during fatiguing stimulation: when the

energy consumption exceeds the production by glycolysis and oxidative phosphorylation, breakdown of PCr will start immediately whereas ATP degradation will not occur until the concentration of PCr has reached a very low level (Carlson & Wilkie, 1974; Allen & Orchard, 1987). On this scenario the initial part of fatigue

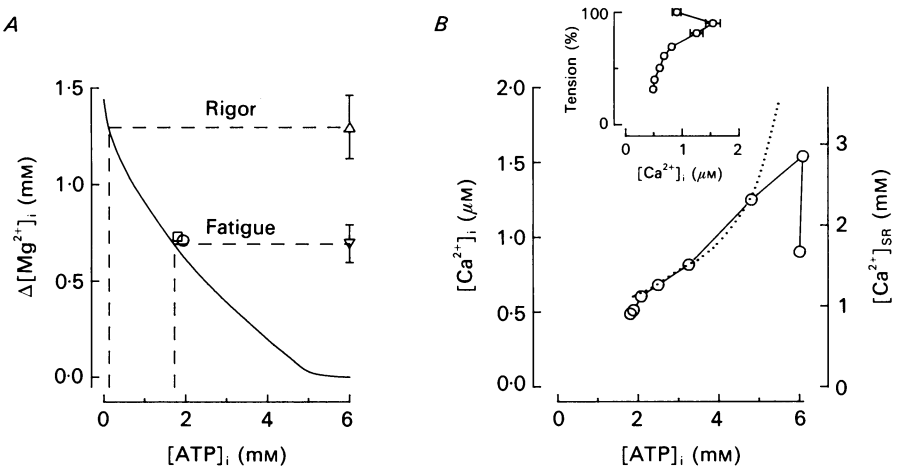

Fig. 9. Panel *A* shows the calculated relation between $\Delta[Mg^{2+}]_i$ and $[ATP]_i$. The curve was obtained by modelling the relation between $\Sigma[Mg^{2+}]_i$ and $[Mg^{2+}]_i$ at several $[ATP]_i$ ranging from 0 to 6 mM (cf. dashed lines in Fig. 8). The $\Delta[Mg^{2+}]_i$ was measured at a $\Sigma[Mg^{2+}]_i$ of 7·07 mM (the $\Sigma[Mg^{2+}]_i$ giving the resting $[Mg^{2+}]_i$; dotted line in Fig. 8) and plotted against $[ATP]_i$. ▽ and △ represent the mean (±S.E.M.) $\Delta[Mg^{2+}]_i$ measured in fatigue and rigor, respectively; the dashed lines give the modelled $[ATP]_i$ in the respective case. Two variations of the basic model have been performed at the $[ATP]_i$ in fatigue: □ was obtained by including 2·3 mM-IMP and ○ was obtained by increasing the resting $[Ca^{2+}]_i$ from 30 to 100 nM. Neither of these alterations had a marked effect. Panel *B* shows the modelled relation between $[ATP]_i$ and tetanic $[Ca^{2+}]_i$ (○——○) which was constructed from an $[ATP]_i$ *vs.* tension curve and a tetanic $[Ca^{2+}]_i$ *vs.* tension curve by substituting for tension. The relation between $[ATP]_i$ and tension was obtained by combining Figs 4*A* and 9*A* and substituting for $\Delta[Mg^{2+}]_i$. The inset in *B* shows the relation between tetanic $[Ca^{2+}]_i$ and tension obtained during fatigue runs in the present preparation ($n = 8$; values obtained by reanalysing data from Westerblad & Allen, 1991). Panel *B* also shows the relation between $[ATP]_i$ and the free $[Ca^{2+}]$ in the SR ($[Ca^{2+}]_{SR}$) (dotted line). $[Ca^{2+}]_{SR}$ was established as follows. The free energy of ATP hydrolysis (ΔG_{ATP}) was calculated as:

$$\Delta G_{ATP} = \Delta G^{o} + RT \ln ([ATP][ADP]^{-1}[P_i]^{-1}),$$

where ΔG^{o} was obtained from Alberty (1968; $[Mg^{2+}]$ 1·0 mM, pH 7·3) and equals 37 kJ/mol. (Formally ΔG_{ATP} and ΔG^{o} are negative quantities but we have for simplicity reversed their signs in the present equations.) R and T have their usual meanings. The concentrations of ATP, ADP, and P_i were obtained from our model. The $[Ca^{2+}]_{SR}$ was then calculated on the assumption that one molecule of ATP pumps two Ca^{2+} into the SR and that the free energy of ATP hydrolysis provides the work for this operation:

$$[Ca^{2+}]_{SR} = [Ca^{2+}]_i \exp(\Delta G_{ATP}/RT),$$

where $[Ca^{2+}]_i$ is the concentration at rest which was obtained from Westerblad & Allen (1991).

runs represents the period when the concentration of PCr is declining, which does not have any significant effect on $[Mg^{2+}]_i$, and the final part represents a period of falling $[ATP]_i$, which elevates $[Mg^{2+}]_i$.

One aim of the present study was to find out if the final rapid tension decline in fatigue runs (phase 3) was caused by Mg^{2+} inhibition of SR Ca^{2+} release. We found a reasonable temporal correlation between the final tension decline and increasing $[Mg^{2+}]_i$ which supports this hypothesis. However, the experiments with $MgCl_2$ injection appear to disprove the hypothesis. It is clear from Fig. 7*B* that elevated $[Mg^{2+}]_i$ depresses tetanic tension in unfatigued fibres, possibly by inhibiting SR Ca^{2+} release, and the $[Mg^{2+}]_i$ which reduces tension to 0·5 P_o is about 2·9 mM. Using skinned fibres with intact voltage-sensor control of SR Ca^{2+} release, Lamb & Stephenson (1991) showed a significant inhibition of SR Ca^{2+} release between 1 and 3 mM-Mg^{2+}. It thus appears safe to conclude that an elevation of $[Mg^{2+}]_i$ impairs the SR Ca^{2+} release, but the increase of $[Mg^{2+}]_i$ in fatigue is too small to explain a decline in $[Ca^{2+}]_i$ of the magnitude observed in fatigued fibres (Westerblad & Allen, 1991).

$[ATP]_i$ *in fatigue and rigor*

We found a striking temporal correlation between the rise in $[Mg^{2+}]_i$, on the one hand, and the final tension decline in both fatigue and metabolic blockade, on the other. Furthermore, there was a correlation between recovery of $[Mg^{2+}]_i$ and tetanic tension after fatigue runs. Since the tension reduction cannot be explained by direct effects of high $[Mg^{2+}]_i$, it may instead be related to mechanisms underlying the rise in $[Mg^{2+}]_i$: insufficient energy supply leading to reduced $[ATP]_i$. We have employed modelling to determine the likely change in $[ATP]_i$ for the observed changes in $[Mg^{2+}]_i$. As mentioned above, a reasonable agreement was found between modelled and measured values of $[Mg^{2+}]_i$ buffering and $[Mg^{2+}]_i$ changes due to alkalinization. The metabolic blockade experiments can also be used to test the model: the increase of $[Mg^{2+}]_i$ in rigor should be similar to that predicted by the model when $[ATP]_i$ is reduced from the rested level (6 mM) to close to zero. Figure 9*A* shows the modelled relationship between $[ATP]_i$ reduction and $[Mg^{2+}]_i$ rise. The curve was obtained by reducing $[ATP]_i$ stepwise while calculating the concentrations of PCr, ADP, AMP, and P_i (for details see Methods) and while keeping the $\Sigma[Mg^{2+}]_i$ constant at the value giving the measured resting $[Mg^{2+}]_i$ (indicated by the dotted line in Fig. 8). It can be seen in Fig. 9*A* that the model predicts a $\Delta[Mg^{2+}]_i$ of about 1·45 mM at zero ATP which compares with the measured 1·30 mM rise in rigor. One explanation for this discrepancy is as follows. We assumed that complete breakdown of ATP and PCr produced 37 mM-P_i and that P_i mostly existed in the free form. Of the 6 mM-Mg^{2+} released from ATP in rigor, most ($\sim$ 3·4 mM) is bound to P_i in our model. However, since IAA is known to inhibit glycolysis (Carlson & Siger, 1959), phosphorylated metabolites in the glycolytic pathway would accumulate in our metabolic blockade experiments (cf. Pirolo & Allen, 1986). Martell & Smith (1974) list two of these metabolites (glucose-1-phosphate and fructose-1,6-diphosphate) and both bind Mg^{2+} more strongly than free P_i. If it is generally true that the phosphorylated metabolites bind more Mg^{2+} than free P_i, this would give a $[Mg^{2+}]_i$ in rigor which is lower than that predicted by our model.

The modelled $[ATP]_i$ for the average $[Mg^{2+}]_i$ in fatigue was 1·74 mM, i.e. $[ATP]_i$ was reduced to about 30% of the original. This $[ATP]_i$ is lower than most values reported in the literature (for review see Vøllestad & Sejersted, 1988). We suggest the following explanation for this difference. Values of the $[ATP]_i$ in fatigue have often been obtained with biochemical techniques on isolated animal muscles or human

muscle samples obtained from biopsies; alternatively, NMR (nuclear magnetic resonance) technique has been used on human or animal muscle *in vivo* or whole muscle preparations *in vitro*. In such studies involving whole muscles or muscle groups it is likely that marked alteration of the extracellular fluid would occur. In the

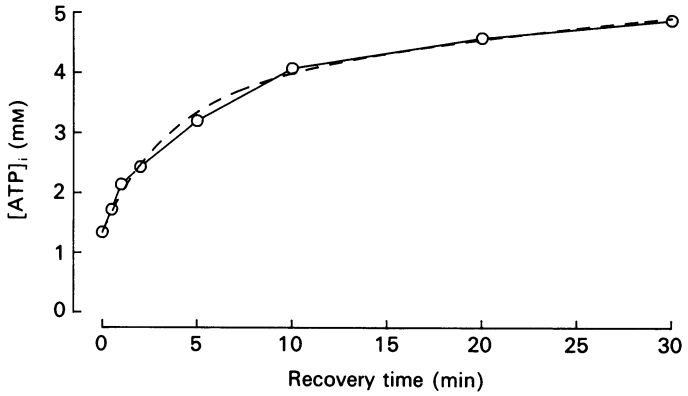

Fig. 10. Recovery of $[ATP]_i$ after fatiguing stimulation. The $[ATP]_i$ *vs.* $\Delta[Mg^{2+}]_i$ relation of Fig. 9*A* was used to convert mean values of $\Delta[Mg^{2+}]_i$ in Fig. 5 to $[ATP]_i$. Recovery of $[ATP]_i$ could be described by an equation with two exponential functions:

$$[ATP]_i = [ATP]_{fat} + [ATP]_1(1-\exp(-t/\tau_1)) + [ATP]_2(1-\exp(-t/\tau_2)),$$

where $[ATP]_{fat}$ is the $[ATP]_i$ in fatigue and t is the time from the end of fatiguing stimulation. The last two variables in the equation describe two pools of metabolites which recover with the time constants τ_1 and τ_2, respectively. $[ATP]_i$ in fatigue was, in these fibres, 1·34 mM. The best curve fit was obtained with the following values: $[ATP]_1$ = 2·12 mM, $[ATP]_2$ = 2·54 mM, τ_1 = 3·25 min, and τ_2 = 35·4 min.

present study, on the other hand, the extracellular milieu was kept constant by continuously superfusing the fibre with fresh solution. Thus extracellular factors, such as accumulation of potassium ions or lactic acid, may limit the performance of whole muscles before a marked reduction of $[ATP]_i$ develops.

Our way of converting changes of $[Mg^{2+}]_i$ into $[ATP]_i$ is simplified in that $[Ca^{2+}]_i$ was held constant. We have previously shown that the resting $[Ca^{2+}]_i$ increases from about 30 nM at rest to about 100 nM in fatigue (Westerblad & Allen, 1991). However, such an increase of $[Ca^{2+}]_i$ only had a small effect on the modelled relation between $[Mg^{2+}]_i$ and $[ATP]_i$ (○ in Fig. 9*A*).

Recovery of $[ATP]_i$

The values of $\Delta[Mg^{2+}]_i$ obtained during recovery (Fig. 5) has been translated into $[ATP]_i$ in Fig. 10. The recovery of $[ATP]_i$ obtained in this way can be described by two exponential functions (dashed line in Fig. 10) which suggests that two pools of metabolites had been formed, one which recovered relatively fast ($t_{0.5} \sim 2.2$ min) and one which recovered more slowly ($t_{0.5} \sim 24$ min). These two pools were of similar size: the rapidly and slowly recovering pools amounted to about 45 and 55% of the ATP which broke down during fatigue runs, respectively. The rapidly recovering pool probably represents rephosphorylation of ATP from AMP and ADP. The other pool

recovered with a time course similar to that observed for restoration of ATP from IMP (Meyer & Terjung, 1979), which is slow because it involves reamination of IMP to AMP. Thus these results suggest that a large fraction of the AMP produced during fatigue runs was deaminated to IMP: of the 4·2 mM-ATP which broke down during fatigue runs about 2·3 mM would form IMP. In our basic modelling we have assumed that no IMP was formed and this may cause an error in our estimate of $[ATP]_i$ in fatigue. However, inclusion of IMP in the model only resulted in a minor change of $[ATP]_i$ in fatigue (□ in Fig. 9*A*).

The role of insufficient energy supply in fatigue

We have previously shown that the $[Ca^{2+}]_i$ during tetanus falls during the final phase of fatigue runs (Westerblad & Allen, 1991) and the present results suggest this fall to be caused by some mechanism related to ATP breakdown. Figure 9*B* illustrates the relation between $[ATP]_i$ and tetanic $[Ca^{2+}]_i$ during fatigue runs (for details see figure legend). It can be seen that after an initial increase of tetanic $[Ca^{2+}]_i$, which we attribute to reduced myoplasmic Ca^{2+} buffering (Westerblad & Allen, 1991), there was a correlation between declining tetanic $[Ca^{2+}]_i$ and $[ATP]_i$. What mechanisms may couple ATP degradation to reduced SR Ca^{2+} release? We consider two possible mechanisms in greater detail: (i) inhibition of the SR Ca^{2+} release channels and (ii) reduced SR Ca^{2+} content.

(i) The function of the SR Ca^{2+} release chanels is impaired at very low [ATP] (apparent K_M (Michaelis–Menten constant) ~ 1 mM; Meissner *et al.* 1986). However, any adenine nucleotide appears to be effective in activating SR Ca^{2+} release (Morii & Tonomura, 1983; Smith, Coronado & Meissner, 1985; Meissner *et al.* 1986). Our results suggest that there was a reduction of the total concentration of adenine nucleotides in fatigue (see above), but this reduction was probably not big enough to markedly affect SR Ca^{2+} release. It is, however, possible that the combination of high $[Mg^{2+}]_i$ and a reduction of the total adenine nucleotide pool significantly inhibits SR Ca^{2+} release.

Degradation of ATP will result in an accumulation of AMP which may be deaminated to IMP and NH_3 (Sahlin *et al.* 1978; Meyer & Terjung, 1979). Morii & Tonomura (1983) showed that nucleotides other than adenine nucleotides did not accelerate SR Ca^{2+} release. Furthermore, these authors showed that cytosine triphosphate (CTP) inhibited adenine nucleotide-induced activation of Ca^{2+} release. If IMP exerts an effect on SR Ca^{2+} release similar to that of CTP, this may provide a link between ATP degradation and declining tetanic $[Ca^{2+}]_i$. We are not aware of any study which may support or disprove this hypothesis.

(ii) The SR Ca^{2+} pumps require energy and impaired pumping will result in reduced SR Ca^{2+} content. We have previously shown that in the present preparation the tetanic $[Ca^{2+}]$ in the presence of caffeine is markedly smaller in fatigue than in control. If it is assumed that maximum Ca^{2+} release occurs during tetanic stimulation in caffeine, this result indicates a reduced SR Ca^{2+} content in fatigue (for discussion see Westerblad & Allen, 1991).

The maximum Ca^{2+} gradient between the myoplasm and the SR that can be achieved by these pumps depends on the free energy of ATP hydrolysis (ΔG_{ATP}). The dotted line in Fig. 9*B* represents a calculation of the maximum free $[Ca^{2+}]$ in the SR

($[Ca^{2+}]_{SR}$) during fatigue (for details of calculation see figure legend). The $[Ca^{2+}]_{SR}$ axis has been chosen so that the line passes through the third $[ATP]_i$–$[Ca^{2+}]_i$ data point; thus the initial increase of $[Ca^{2+}]_i$, which we attribute to reduced Ca^{2+} buffering, has been ignored. When plotted in this way, there is a good correlation between reduced tetanic $[Ca^{2+}]_i$ and $[Ca^{2+}]_{SR}$. A possible scenario would then be that the opening of SR Ca^{2+} channels remains constant in fatigue but the released Ca^{2+} declines due to a reduced Ca^{2+} gradient between the SR and myoplasm.

The observed relation between $[Mg^{2+}]_i$ and tetanic tension during fatigue was similar to that during recovery which suggests a common underlying mechanism. The suggested inhibition of the SR Ca^{2+} channels (see (i) above) may be applied to both fatigue and recovery conditions. However, the mechanism involving reduced $[Ca^{2+}]_{SR}$ (see (ii) above) cannot be applied to the recovery if a substantial IMP formation is assumed, because in this case ΔG_{ATP} would recover more rapidly than $[ATP]_i$.

It should be noted that there are several other mechanisms which may link declining $[ATP]_i$ to reduced Ca^{2+} release; for instance, the function of the Na^+–K^+ pumps is energy dependent and impaired function of these pumps may cause action potential failure. Furthermore, a reduction of $[ATP]_i$ increases the opening of ATP-regulated K^+ channels (Spruce, Standen & Stanfield, 1987), which will tend to clamp the membrane potential at the equilibrium potential for K^+ and consequently reduce the amplitude of action potentials.

We thank Dr Simeon Cairns for useful discussion. The study was supported by grants from the Australian National Health and Medical Research Council. H.W. acknowledges support from the Rolf Edgar Lake Postdoctoral Fellowship, the Swedish Medical Research Council, and the Swedish Society of Medicine (SLS).

REFERENCES

ALBERTY, R. A. (1968). Effect of pH and metal ion concentration on the equilibrium hydrolysis of adenosine triphosphate to adenosine diphosphate. *Journal of Biological Chemistry* **243**, 1337–1343.

ALLEN, D. G., CAIRNS, S. P. & WESTERBLAD, H. (1992). Intracellular Mg^{2+} in fatigue of isolated mouse muscle fibres. Abstract to the European Muscle Club, XX Annual Meeting, Oxford, UK. *Journal of Muscle Research and Cell Motility* (in the Press).

ALLEN, D. G. & ORCHARD, C. H. (1987). Myocardial contractile function during ischemia and hypoxia. *Circulation Research* **60**, 153–168.

BAKER, P. F. & CRAWFORD, A. C. (1972). Mobility and transport of magnesium in squid giant axons. *Journal of Physiology* **227**, 855–874.

BLATTER, L. A. (1990). Intracellular free magnesium in frog skeletal muscle studied with a new type of magnesium-selective microelectrode: interactions between magnesium and sodium in the regulation of $[Mg^{2+}]_i$. *Pflügers Archiv* **416**, 238–246.

CARLSON, F. D. & SIGER, A. (1959). The creatine phosphotransfer reaction in iodoacetate-poisoned muscle. *Journal of General Physiology* **43**, 301–313.

CARLSON, F. D. & WILKIE, D. R. (1974). *Muscle Physiology*. Prentice-Hall, Englewood Cliffs, NJ, USA.

CURTIN, N. A. & WOLEDGE, R. C. (1978). Energy changes and muscular contraction. *Physiological Reviews* **58**, 690–761.

FABIATO, A. (1988). Computer programs for calculating total from specified free or free from specified total ionic concentrations in aqueous solutions containing multiple metals and ligands. *Methods in Enzymology* **157**, 378–417.

GODT, R. E. & MAUGHAN, D. W. (1988). On the composition of the cytosol of relaxed skeletal muscle of the frog. *American Journal of Physiology* **254**, C591–604.

GRYNKIEWICZ, G., POENIE, M. & TSIEN, R. Y. (1985). A new generation of Ca^{2+} indicators with greatly improved fluorescence properties. *Journal of Biological Chemistry* **260**, 3440–3450.

GÜNZEL, D. & GALLER, S. (1991). Intracellular free Mg^{2+} concentration in skeletal muscle fibres of frog and crayfish. *Pflügers Archiv* **417**, 446–453.

HU, Z., BÜHRER, T., MÜLLER, M., RUSTERHOLZ, B., ROUILLY, M. & SIMON, W. (1989). Intracellular magnesium ion-selective microelectrodes based on a neutral carrier. *Analytical Chemistry* **61**, 574–576.

KONISHI, M., HOLLINGWORTH, S., HARKINS, A. B. & BAYLOR, S. M. (1991). Myoplasmic calcium transients in intact frog skeletal muscle fibers monitored with the fluorescent indicator furaptra. *Journal of General Physiology* **97**, 271–301.

KONISHI, M., OLSON, A., HOLLINGWORTH, S. & BAYLOR, S. M. (1988). Myoplasmic binding of fura-2 investigated by steady-state fluorescence and absorbance measurements. *Biophysical Journal* **54**, 1089–1104.

KRAUSE, S. M. (1991). Effect of increased free $[Mg^{2+}]_i$ with myocardial stunning on sarcoplasmic reticulum Ca^{2+}-ATPase activity. *American Journal of Physiology* **261**, H229–235.

LAMB, G. D. & STEPHENSON, D. G. (1991). Effect of Mg^{2+} on the control of Ca^{2+} release in skeletal muscle fibres of the toad. *Journal of Physiology* **434**, 507–528.

LÄNNERGREN, J. & WESTERBLAD, H. (1987). The temperature dependence of isometric contractions of single, intact fibres dissected from a mouse foot muscle. *Journal of Physiology* **390**, 285–293.

LÄNNERGREN, J. & WESTERBLAD, H. (1991). Force decline due to fatigue and intracellular acidification in isolated fibres from mouse skeletal muscle. *Journal of Physiology* **434**, 307–322.

LEE, J. A., WESTERBLAD, H. & ALLEN, D. G. (1991). Changes in tetanic and resting $[Ca^{2+}]_i$ during fatigue and recovery of single muscle fibres from *Xenopus laevis*. *Journal of Physiology* **433**, 307–326.

LEIJENDEKKER, W. J. & ELZINGA, G. (1990). Metabolic recovery of mouse extensor digitorum longus and soleus muscle. *Pflügers Archiv* **416**, 22–27.

MACDERMOTT, M. (1990). The intracellular concentration of free magnesium in extensor digitorum longus muscle of the rat. *Experimental Physiology* **75**, 763–769.

MARTELL, A. E. & SMITH, R. M. (1974). *Critical Stability Constants*. Plenum Press, New York.

MEISSNER, G., DARLING, E. & EVELETH, J. (1986). Kinetics of rapid Ca^{2+} release by sarcoplasmic reticulum. Effects of Ca^{2+}, Mg^{2+}, and adenine nucleotides. *Biochemistry* **25**, 236–244.

MEYER, R. A. & TERJUNG, R. L. (1979). Differences in ammonia and adenylate metabolism in contracting fast and slow muscle. *American Journal of Physiology* **237**, C111–118.

MORII, H. & TONOMURA, Y. (1983). The gating behavior for Ca^{2+}-induced Ca^{2+} release in fragmented sarcoplasmic reticulum. *Journal of Biochemistry (Tokyo)* **93**, 1271–1285.

PIROLO, J. S. & ALLEN, D. G. (1986). Assessment of techniques for preventing glycolysis in cardiac muscle. *Cardiovascular Research* **20**, 837–844.

RAJU, B., MURPHY, E., LEVY, L. A., HALL, R. D. & LONDON, R. E. (1989). A fluorescent indicator for measuring cytosolic free magnesium. *American Journal of Physiology* **256**, C540–548.

ROBERTSON, S. P., JOHNSON, J. D. & POTTER, J. D. (1981). The time-course of Ca^{2+} exchange with calmodulin, troponin, parvalbumin, and myosin in response to transient increases in Ca^{2+}. *Biophysical Journal* **34**, 559–569.

ROE, M. W., LEMASTERS, J. J. & HERMAN, B. (1990). Assessment of Fura-2 for measurements of cytosolic free calcium. *Cell Calcium* **11**, 63–73.

SAHLIN, K., PALMSKOG, G. & HULTMAN, E. (1978). Adenine nucleotide and IMP contents of the quadriceps muscle in man after exercise. *Pflügers Archiv* **374**, 193–198.

SMITH, J. S., CORONADO, R. & MEISSNER, G. (1985). Sarcoplasmic reticulum contains nucleotide-activated calcium channels. *Nature* **316**, 446–449.

SPRUCE, A. E., STANDEN, N. B. & STANFIELD, P. R. (1987). Studies of the unitary properties of adenosine-5′-triphosphate-regulated potassium channels of frog skeletal muscle. *Journal of Physiology* **382**, 213–236.

VØLLESTAD, N. K. & SEJERSTED, O. M. (1988). Biochemical correlates of fatigue. *European Journal of Applied Physiology* **57**, 336–347.

WESTERBLAD, H. & ALLEN, D. G. (1991). Changes of myoplasmic calcium concentration during fatigue in single mouse muscle fibers. *Journal of General Physiology* **98**, 615–635.

WESTERBLAD, H. & ALLEN, D. G. (1992). Changes of intracellular pH due to repetitive stimulation of single fibres from mouse skeletal muscle. *Journal of Physiology* **449**, 49–71.

WESTERBLAD, H. & LÄNNERGREN, J. (1991). Slowing of relaxation during fatigue in single mouse muscle fibres. *Journal of Physiology* **434**, 323–336.

WILLIAMS, D. A. & FAY, F. S. (1990). Intracellular calibration of the fluorescent calcium indicator Fura-2. *Cell Calcium* **11**, 75–83.